THE JOURNAL OF BIOLOGICAL CHEMISTRY
Vol. 275, No. 31, Issue of August 4, pp. 23540–23548, 2000

Printed in U.S.A.

Nup116p Associates with the Nup82p-Nsp1p-Nup159p Nucleoporin Complex*

Received for publication, March 7, 2000, and in revised form, May 5, 2000
Published, JBC Papers in Press, May 8, 2000, DOI 10.1074/jbc.M001963200

Susanne M. Bailer, Carolin Balduf, Jun Katahira‡, Alexandre Podtelejnikov§, Christiane Rollenhagen¶, Matthias Mann§, Nelly Panté‖, and Ed Hurt**

From the Biochemie-Zentrum Heidelberg, Im Neuenheimer Feld 328, D-69120 Heidelberg, Germany

Nup116p is a GLFG nucleoporin involved in RNA export processes. We show here that Nup116p physically interacts with the Nup82p-Nsp1p-Nup159p nuclear pore subcomplex, which plays a central role in nuclear mRNA export. For this association, a sequence within the C-terminal domain of Nup116p that includes the conserved nucleoporin RNA-binding motif was sufficient and necessary. Consistent with this biochemical interaction, protein A-Nup116p and the protein A-tagged Nup116p C-terminal domain, like the members of the Nup82p complex, localized to the cytoplasmic side of the nuclear pore complex, as revealed by immunogold labeling. Finally, synthetic lethal interactions were found between mutant alleles of *NUP116* and all members of the Nup82p complex. Thus, Nup116p consists of three independent functional domains: 1) the C-terminal part interacts with the Nup82p complex; 2) the Gle2p-binding sequence interacts with Gle2p/Rae1p; and 3) the GLFG domain interacts with shuttling transport receptors such as karyopherin-β family members.

The nuclear pore complex (NPC)[1] is a huge organelle with an intricate structure of octagonal symmetry (for review, see Ref. 1). It allows passive diffusion of small molecules and controls active transport of macromolecules in and out of the nucleus. Of the estimated proteins constituting the NPC, almost all have been identified in the case of the yeast *Saccharomyces cerevisiae* (2). In subsequent studies, their nearest neighborhood was analyzed by characterizing their biochemical organization into subcomplexes or by immunolocalizing them to distinct sites within the structural framework of the NPC (for review, see Ref. 1). Following the elucidation of the Ran cycle, which drives vectorial nucleocytoplasmic transport, and the discovery of the shuttling importin/karyopherin-β transport receptor family together with their cargoes, interest is now focusing on the understanding of the actual transport mechanism through the NPCs (for review, see Ref. 3)

In yeast, several NPC subcomplexes are known. The Nup84p complex has functions in both NPC biogenesis and nuclear mRNA export (4–7). The Nup170p-Nup157p-Nup188p complex may functionally contribute to transport processes and structural integrity of the NPC as well as to cell cycle control (8–10).

Nsp1p is unique compared with other nucleoporins in that it forms two distinct NPC subcomplexes. The first one isolated is the Nsp1p-Nup49p-Nup57p-Nic96p complex involved in nuclear protein import and localized to the nucleoplasmic and cytoplasmic face of the central gated channel and to the nuclear basket (11–13). The higher eucaryotic NPC subcomplex p62-p54-p58/p45 with its associated NUP93 shows striking homology to this Nsp1p subcomplex (14–17). The second Nsp1p complex is formed by Nup82p and Nup159p (18–20). As with the Nic96p complex, all components are essential and tethered to each other via their C-terminal coiled-coil domains. Temperature-sensitive mutants of Nup82p and Nup159p display severe defects in nuclear mRNA export, but not in nuclear protein import (18, 20–22). While Nup159p-N seems to be involved in mRNA export, the C-terminal domains of Nup159p and Nup82p are required for stable subcomplex formation and their integration into the NPC (19, 20, 23). The Nup82p complex most likely represents the yeast counterpart of the higher eucaryotic CAN/NUP214-NUP88/84-p66-CRM1 complex (24, 25).

Several proteins involved in nuclear mRNA export have been shown or are likely to interact with the Nup82p or CAN/NUP214 complex. TAP, the higher eucaryotic homologue of yeast Mex67p, a transport factor essential for mRNA export, interacts with the CAN/NUP214 FG repeat region (26–28). Recently, the N-terminal part of Nup159p was found to directly interact with Dbp5p, an ATP-driven RNA helicase (29, 30). Gle1p, an essential nuclear export signal containing protein involved in mRNA export, acts as a high copy suppressor of C-terminal temperature-sensitive mutations in Nup159p and Nup82p (20, 31, 32) and is a good candidate to bind to the Nup82p complex via Dbp5p (29, 33). In addition, *GLE1* is synthetically lethal with *NUP116* and *NUP100* (31). Taken together, since the Nup82p complex is exclusively localized to the cytoplasmic side of the NPC and interacts with the above-mentioned proteins involved in mRNA transport, its components are likely to play a crucial role in mRNA export steps through the NPCs and possibly release of the transport cargo into the cytoplasm.

Nup116p is a nucleoporin that was initially found to be genetically linked to Nsp1p (34) and that shows homology to Nup100p and Nup145p-N over its entire length (35–38). Nup116p, Nup100p, and Nup145p-N share (i) an N-terminally located GLFG repeat domain, previously shown to bind karyo-

* The costs of publication of this article were defrayed in part by the payment of page charges. This article must therefore be hereby marked "*advertisement*" in accordance with 18 U.S.C. Section 1734 solely to indicate this fact.

‡ Present address: Project Research for Molecular Microbiology, Research Inst. for Microbial Diseases, Osaka University, 31 Yamada-oka, Suita, Osaka 565, Japan.

§ Present address: CEBI Odense University, Staermosegaardsvej 16, DK-5230 Odense, Denmark.

¶ Present address: Swiss Federal Inst. of Technology, Universitätsstr. 16, 8092 Zürich, Switzerland.

‖ Present address: Dept. of Zoology, University of British Columbia, 6270 University Blvd., Vancouver, BC V6T 1Z4, Canada.

** Recipient of Deutsche Forschungsgemeinschaft Grant SFB352. To whom correspondence should be addressed. Tel.: 49-6221-544173; Fax: 49-6221-544369; E-mail: cg5@ix.urz.uni-heidelberg.de.

[1] The abbreviations used are:NPC, nuclear pore complex; -N and -C, N- and C-terminal domains, respectively; NRM, nucleoporin RNA-binding motif; GLEBS, Gle2p-binding sequence; PCR, polymerase chain reaction; ProtA, protein A; GFP, green fluorescent protein; PAGE, polyacrylamide gel electrophoresis.

TABLE I
Yeast strains

Strain	Genotype	Ref.
RS453	*Mat***a**/α, *ade2/ade2, his3/his3, leu2/leu2, trp1/trp1, ura3/ura3*	Segref *et al.* (26)
BJ2168	*Mat***a**, *leu2, trp1, ura3-52, pep4-3, pre1-407, prb1-1122*	Aris and Blobel (59)
nup116Δ(URA3)	*Mat*α, *ade2, his3, leu2, trp1, ura3, nup116*::*URA3*	Fabre *et al.* (38)
nup116Δ(HIS3)	*Mat*α, *ade2, his3, leu2, trp1, ura3, nup116*::*HIS3*	This study
LGY106	*Mat***a**, *ura3–52, leu2Δ1, his3Δ200, nup159*::*HIS3* (pLG4-URA3-NUP159 CEN)	Gorsch *et al.* (55)
nup100Δ	*Mat***a**, *ade2, his3, leu2, trp1, ura3, nup100*::*LEU2*	Fabre *et al.* (38)
nup82Δ	*Mat***a**, *ade2, his3, leu2, trp1, ura3, nup82*::*HIS3* (pRS316-URA3-NUP82)	Grandi *et al.* (18)
nup145Δ	*Mat***a**, *ura3-Δ851, trp1 Δ63, leu2 Δ1, nup145*::*HIS3* (pRS316-URA3-NUP145)	Teixeira *et al.* (7)
nup82Δ/nup116Δ	*Mat*α, *ade2, his3, leu2, trp1, ura3, nup116*::*HIS3 nup82*::*HIS3* (pRS316-URA3-NUP82)	This study
nsp1Δ/nup116Δ	*Mat*α, *ade2, his3, leu2, trp1, ura3, nup116*::*HIS3 nsp1*::*HIS3* (pRS316-URA3-NSP1)	This study
nup159Δ/nup116Δ	*Mat***a**, *his3, leu2, trp1, ura3, nup116*::*HIS3 nup159*::*HIS3* (pLG4-URA3-NUP159 CEN)	This study
nup82Δ/nup100Δ	*Mat*α, *ade2, his3, leu2, trp1, ura3, nup100*::*LEU2 nup82*::*HIS3* (pRS316-URA3-NUP82)	This study
JU4-2xJR26-19B/ProtA-DHFR[a]	*Mat***a**/α, *ade2-1/ade2-1, ade8/ADE8, can1-100/can1-100, his4/HIS4, his3/HIS3, leu2-3/leu2-3, lys1-1/lys1-1, ura3-52/ura3-52* (pYep13-ProtA-DHFR)	Nehrbass *et al.* (60)

[a] DHFR, dihydrofolate reductase.

pherin-β-like transport factors (39, 40), and (ii) a conserved C-terminal domain that includes the nucleoporin RNA-binding motif (NRM) shown to bind to homopolymeric RNA *in vitro* and to perform a redundant function (38). Nup116p, however, differs from Nup100p and Nup145p-N by harboring an evolutionarily conserved sequence of ~60 amino acids called the Gle2p-binding sequence (GLEBS), which mediates stable complex formation with Gle2p (41, 42). Disruption of either *GLE2* or *NUP116* leads to temperature sensitivity and a concomitant defect in nuclear poly(A)$^+$ RNA export (36, 43). For *nup116Δ* cells, an additional defect in tRNA export was reported (44); it is not clear, however, whether these RNA transport defects are direct or merely due to sealed nuclear pores observed in these mutants (36, 41, 43). The fact that the Gle2p homologue in *Schizosaccharomyces pombe*, Rae1p, is essential for mRNA export (45, 46) strongly points to a direct role of this protein in RNA transport processes. NUP98, the putative higher eucaryotic homologue of Nup116p, also carries a GLEBS in its N-terminal half where GLE2/RAE1 docks and a C-terminally located NRM (47–50). Microinjection of polyclonal anti-NUP98 antibodies into *Xenopus* oocytes blocks nuclear export of several types of RNAs (49), whereas overexpression of the NUP98 GLEBS in tissue culture cells results in nuclear retention of poly(A)$^+$ RNA (50). Finally, a role of NUP98 in nuclear export of human immunodeficiency virus-1 Rev was also suggested (51). NUP98, which is preferentially located on the nucleoplasmic side of the NPC, could represent a more mobile nucleoporin that shuttles between the nucleus and cytoplasm together with its associated GLE2/RAE1 (48, 50–52).

To further understand the function of Nup116p, Nup100p, and Nup145p-N within the structural framework of the NPCs, we aimed to define their physical and functional interaction with other nucleoporins. Previously, we showed that Nup116p is targeted to the NPC via its C-terminal domain (41). We demonstrate here that Nup116p is predominantly localized to the cytoplasmic side of the NPC, where it physically and genetically interacts with the Nup82p-Nsp1p-Nup159p complex via its C-terminal domain including the NRM. Our genetic data support the idea that Nup116p consists of at least three independent functional domains, of which the C-terminal part interacts with the Nup82p complex, the GLEBS with Gle2p/Rae1p, and the GLFG domain with shuttling transport receptors such as the karyopherin-β family.

MATERIALS AND METHODS

Yeast Strains and Growth, Microbiological Techniques, and Plasmids—The yeast strains used in this work are listed in Table I. Microbiological techniques, plasmid transformation, mating, sporulation of diploids, and tetrad analysis were done essentially as described (6). DNA manipulations (restriction analysis, end-filling reactions, ligations, PCR amplifications, etc.) were carried out essentially as described (58).

Plasmids—All fusion constructs, which were tagged amino-terminally with either two IgG-binding domains derived from *Staphylococcus aureus* ProtA, green fluorescent protein (GFP) or Myc, were expressed under the control of the *NOP1* promoter. The *NSP1* construct is exceptional since it is expressed under the control of the alcohol dehydrogenase promoter and does not carry a tag. All constructs contained authentic 3′-noncoding sequences except for pRS315-ProtA-NUP98-(498–920), which contains a *NUP116* 3′-noncoding region, and pRS414-GFP-NUP159-(2–1460), which contains an alcohol dehydrogenase 3′-noncoding region. Expression of all fusion proteins was verified by Western blot analysis using commercially available anti-ProtA, anti-GFP, or anti-Myc antibodies. The constructs are listed in Table II.

Disruption of NUP116—For complete disruption of the *NUP116* open reading frame, a disruption cassette was designed where two PCR fragments consisting of 300 base pairs of *NUP116* 5′-untranslated region including the *NUP116* ATG codon (*Xba*I-*Bam*HI) and the *NUP116* stop codon followed by 300 base pairs of 3′-untranslated region (*Bam*HI-*Apa*I) were ligated into pBluescript. The *HIS3* gene was inserted at the *Bam*HI site. pBluescript-*nup116Δ(HIS3)* was cut using *Xba*I-*Apa*I to release *nup116Δ(HIS3)*, which was used to transform the diploid strain RS453. Heterozygous HIS$^+$ transformants were analyzed for correct integration at the *NUP116* locus by PCR. After sporulation, haploid *nup116Δ(HIS3)* progeny were isolated that were temperature-sensitive for growth at 37 °C.

Mutagenesis of NUP82—Temperature-sensitive alleles of *NUP82* mapping in the N-terminal region were generated according to published methods (56). A unique *Nhe*I site was introduced by PCR just before the putative coiled-coil domain of the *NUP82* gene (at codon 521 by changing agt to agc), and the resulting DNA fragments were subcloned into pRS315-pNOP-ProtA. The resulting plasmid was cut at the unique *Nsi*I and *Nhe*I sites, which releases a DNA fragment encoding amino acids 108–519 of Nup82p. The gapped vector was transformed into the *NUP82* shuffle strain along with PCR fragments encoding amino acids 2–626 of Nup82p that had been amplified under mutagenic conditions (57). Transformants were selected on SDC-Leu; subsequently, the wild-type plasmid was shuffled out on 5-fluoroorotic acid. 5-Fluoroorotic acid survivors were restreaked on YPD plates and selected for temperature-sensitive growth at 37 °C. Plasmids were isolated from such temperature-sensitive mutants and analyzed further.

Antibodies—To detect the Myc tag, the monoclonal anti-c-Myc antibody-2 (9E10.3, culture supernatant; Neomarkers, Fremont, CA) was

TABLE II
Plasmids

Plasmid	Comments	Ref.
pRS414-ProtA-NUP116-(Δ1–58)	The construct is called *NUP116* in Fig. 5.	Bailer *et al.* (41)
pRS414-ProtA-NUP116-(706–1113)	The construct encodes ProtA-Nup116p-C.	Bailer *et al.* (41)
pRS414-ProtA-NUP100-(559–959)	The construct encodes ProtA-Nup100p-C.	This study
pRS315-ProtA-NUP145-(247–605)	The construct encodes ProtA-Nup145p-NΔGLFG.	Teixeira *et al.* (7)
pRS315-ProtA-NUP116-(706–854)		This study
pRS315-ProtA-NUP116-(855–966)		This study
pRS315-ProtA-NUP116-(967–1113)		This study
pRS315-ProtA-NUP116-(855–1113)	The 5th–8th constructs encode parts of Nup116p-C.	This study
pRS314-GFP-NUP116-(706–1113)	The construct is called *NUP116-C* in Fig. 5.	Bailer *et al.* (41)
pRS414-GFP-NUP100-(559–959)	The construct encodes GFP-Nup100p-C.	This study
pRS414-ProtA-NUP116-(59–705)	The construct is called *nup116ΔC* in Fig. 5.	Bailer *et al.* (41)
pRS414-ProtA-NUP116-(Δ110–166)	The construct is *nup116ΔGLEBS* in Fig. 5.	Bailer *et al.* (41)
pRS414-ProtA-NUP116-(Δ923–1113)	The construct is called *nup116ΔNRM* in Fig. 5.	This study
pRS316-NUP82		Grandi *et al.* (18)
pCH1122-URA3-ADE3-NSP1		Wimmer *et al.* (34)
YCplac33-URA3-NUP159 (pLG4)		Del Priore *et al.* (22)
pSB32-pADH-NSP1-L640S	The construct is called *nsp1-L640S* in Fig. 5.	Wimmer *et al.* (34)
pUN100-ProtA-TEV-NUP82	This construct is called *NUP82* in Fig. 5*B*.	This study
pRS315-ProtA-*nup82-27*	This construct is called *nup82-27* in Fig. 5*B*.	This study
pRS315-GFP-NUP82-(2-713)		This study
YCplac111-LEU2-NUP159 (pLG1)	This construct is called *NUP159* in Fig. 5.	Gorsch *et al.* (55)
YCplac111-LEU2-*rat7-1*/*nup159-1* (pSD3)	This construct is called *nup159-1* in Fig. 5.	Del Priore *et al.* (22)
YCplac111-LEU2-NUP159ΔRep (pAM1)	This construct is called *nup159ΔRep* in Fig. 5.	Del Priore *et al.* (22)
YCplac111-LEU2-NUP159ΔN (pVDP16)	This construct is called *nup159ΔN* in Fig. 5.	Del Priore *et al.* (22)
YCplac111-LEU2-NUP159-C (pVDP17)	This construct is called *nup159-C* in Fig. 5.	Del Priore *et al.* (22)
pRS315-GFP-*nup82-27*	Like the 19th construct; ProtA was replaced by GFP.	This study
pRS314-GFP-NUP82-(2–713)	This construct is called *NUP82* in Fig. 5*D*.	This study
pRS314-myc-NUP116-(706–1113)		This study
pRS414-GFP-NUP116-(2–1113)		Bailer *et al.* (41)
pRS414-GFP-NUP159-(2–1460)		This study
pRS314-GFP-NIC96-(2–838)		This study
pRS315-ProtA-NUP98-(498–920)	Using human cDNA of NUP98 as a template, a PCR fragment (*Hind*III-*Apa*I) was generated and fused in frame to a pNOP1-ProtA cassette. A *NUP116* 3′-noncoding region was added.	This study
pRS314-Myc-*nup82–27*	This construct is called *nup82-27* in Fig. 5*D*.	This study

used. To visualize ProtA-tagged proteins, rabbit peroxidase-anti-peroxidase procedure (Dako A/S, Glostrup, Denmark) was used. Ascites fluid of monoclonal antibody 32D6 (a kind gift of J. Aris, University of Florida) was used to detect the C-terminal part of Nsp1p. A rabbit anti-Nup82p antibody[2] was used to visualize Nup82p. The rabbit anti-Nic96p antiserum was as described (11). The anti-Nup159p (No. 4) antiserum raised in guinea pig against the repeat region (55) was kindly provided by C. Cole (Dartmouth Medical School, Hanover NH).

Miscellaneous—Purification of ProtA fusion proteins from yeast, SDS-PAGE, Western blotting, expression and localization of GFP fusion proteins in yeast, and mass spectrometric protein identification were done as described earlier (26). The procedure used for immunodetection of ProtA-tagged proteins using electron microscopy was described previously (13). Minor modifications included spheroplasting using zymolyase for 15 min. To permeabilize the cells, 0.025% Triton X-100 was added to the buffer.

RESULTS

Nup116p Associates with the Nup82p-Nsp1p-Nup159p Complex—The mechanism by which the three related nucleoporins Nup116p, Nup100p, and Nup145p-N (for a schematic drawing of the domain organization, see Fig. 1*A*), which all share a conserved C-terminal domain, interact with other nucleoporins and thereby perform their function in nucleocytoplasmic transport is unknown. We have previously shown that the C-terminal domain of Nup116p can target GFP to the nuclear pores (41). Others have demonstrated that Nup145p-NΔGLFG (which corresponds to the homologous C-terminal domain of the cleaved Nup145p-N protein) also binds to the nuclear envelope (53). We therefore tested whether the C-terminal domain of Nup100p has a similar NPC-targeting activity. Indeed, a GFP-tagged Nup100p-C fusion protein, when expressed in *nup100*Δ cells, exhibited punctuate nuclear envelope staining under a fluorescence microscope, which is typical for an NPC location (Fig. 1*B*). To identify the nucleoporins with which the C-terminal domains of Nup116p, Nup100p, and Nup145p-N interact, their conserved C-terminal domains were tagged with IgG-binding sequences from protein A and expressed in *nup116*, *nup100*, and *nup145* disruption strains, respectively. Following affinity purification by IgG-Sepharose chromatography, the eluted proteins were separated by SDS-PAGE. All three ProtA fusion proteins, which migrated between 60 and 65 kDa, purified equally well and were readily detectable by Coomassie staining (data not shown). Upon silver staining of the gel, less abundant bands became visible, some of which were analyzed by matrix-assisted laser desorption ionization mass spectrometry (Fig. 1*C*). In the case of ProtA-Nup116p-C, a prominent band of 80 kDa was identified as Nup82p (Fig. 1*C*, *lane 2*). Three distinct bands migrating between 100 and 150 kDa were shown by matrix-assisted laser desorption ionization mass spectrometry to correspond to breakdown products of Nup159p (Fig. 1*C*, *lane 2*). Other bands identified were either breakdown products of ProtA-Nup116p-C (migrating at ~30 kDa) or unrelated proteins such as Rpn1p (a 26 S proteasome subunit migrating at ~110 kDa), heat shock proteins (Ssa1p and Ssb1p migrating at ~70 kDa), and Pdc1p (pyruvate decarboxylase-1 migrating at 60 kDa), the latter of which could be contaminants. Surprisingly, neither the ProtA-Nup100p-C nor ProtA-Nup145p-NΔGLFG eluates contained bands that corresponded to Nup82p and Nup159p, although these eluates often exhibited the same contaminating bands as seen for ProtA-Nup116p-C (Fig. 1*C*, *lanes 1* and *3*). Notably, the ProtA-Nup145p-NΔGLFG eluate exhibited two distinct bands at

[2] E. Hurt, unpublished data.

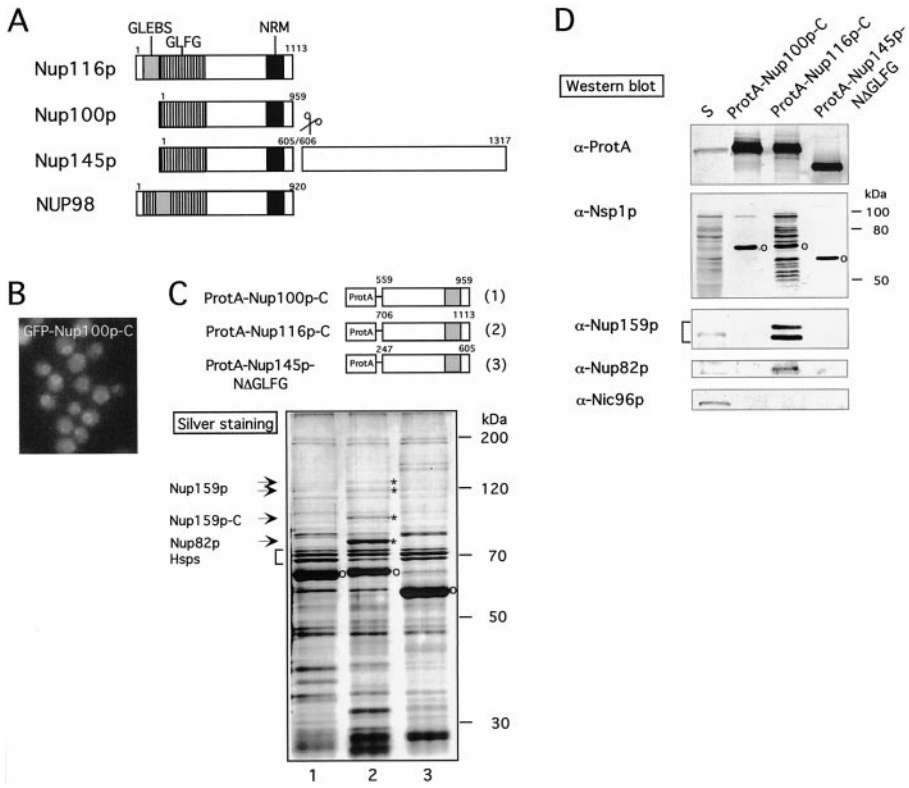

FIG. 1. **Nup116p associates with the Nup82p-Nsp1p-Nup159p complex.** *A*, domain organization of yeast Nup116p, Nup100p, and Nup145p and human NUP98, including the GLEBS, the GLFG region (GLFG repeats), and the NRM. *B*, intracellular localization of GFP-Nup100p-C in a *nup100*Δ strain as revealed by fluorescence microscopy. *C* and *D*, affinity purification of ProtA-Nup100p-C, ProtA-Nup116p-C, and ProtA-Nup145p-NΔGLFG by IgG-Sepharose chromatography. ProtA-Nup100p-C (*lane 1*), ProtA-Nup116p-C (*lane 2*), and ProtA-Nup145p-NΔGLFG (*lane 3*) were analyzed by SDS-PAGE and silver staining (*C*) or Western blotting (*D*). For the Western blots, an aliquot of a whole cell lysate supernatant (*S*) was applied. Copurifying protein bands were identified by mass spectrometric analysis (indicated by *asterisks*). The positions of the ProtA fusion proteins are indicated by *circles*. Western blots were probed with anti-ProtA, anti-Nsp1p, anti-Nup159p, anti-Nup82p, and anti-Nic96p antibodies. *Hsps*, heat shock proteins.

~160 kDa that were absent in the two other eluates. The lower band of this doublet was identified as Nup157p by mass spectrometry (Fig. 1*C*, *lane 3*).

The finding that Nup82p and Nup159p copurified with ProtA-Nup116p-C suggested that Nup116p-C associates with the Nup82p complex consisting of Nup82p, Nup159p, and Nsp1p (18–20). To identify Nsp1p in the ProtA-Nup116p-C eluate, we performed Western blotting using anti-Nsp1p antibodies (Fig. 1*D*). Nsp1p is very unstable during biochemical purification, yielding many breakdown products due to its proteolytic sensitivity (54). However, Nsp1p could clearly be detected in the ProtA-Nup116p-C eluate by immunoblotting. In contrast, Nsp1p was largely absent in the ProtA-Nup100p-C and ProtA-Nup145p-NΔGLFG eluates (Fig. 1*D*). We confirmed by Western analysis that Nup159p and Nup82p copurified with ProtA-Nup116p-C, but not with ProtA-Nup100p-C or ProtA-Nup145p-NΔGLFG (Fig. 1*D*). Nic96p, which served as a negative control, was absent in all three eluates. We conclude that the C-terminal domain of Nup116p, but not the corresponding domains of Nup100p and Nup145p, associates with the Nup82p-Nsp1p-Nup159p complex.

To test whether full-length Nup116p also associates with the Nup82p complex, ProtA-Nup116p was affinity-purified. ProtA-tagged dihydrofolate reductase served as a negative control. The yield of full-length ProtA-Nup116p was lower compared with that of ProtA-Nup116p-C and ProtA-tagged dihydrofolate reductase, which appears to be due to the proteolytic instability of the GLFG repeat region of Nup116p (Fig. 2*A*). Nevertheless, the typical copurifying Nup82p band present in the ProtA-Nup116p-C eluate could also be seen in the ProtA-Nup116p eluate, but was absent in the ProtA-tagged dihydrofolate reductase eluate (Fig. 2*A*, *lanes 1–3*). Western blot analysis confirmed that Nsp1p and Nup159p were present in the ProtA-Nup116p eluate (Fig. 2*A*). In addition, full-length Nup116p strongly associated with Gle2p, which was absent when the C-terminal domain of Nup116p was used as affinity ligand (Fig. 2*A*, *lanes 1* and *2*). Taken together, these data show that the Nup116p-Gle2p complex associates with another nucleoporin subcomplex consisting of Nup82p, Nsp1p, and Nup159p.

To find out which sequence within Nup116p participates in the interaction with the Nup82p complex, different parts of the Nup116p C-terminal domain were tagged with ProtA, expressed in the *nup116*Δ disruption strain, and affinity-purified (Fig. 2*B*). Interestingly, those ProtA-Nup116p constructs that harbor the NRM domain remained associated with all three members of the Nup82p complex (Fig. 2*B*, *lanes 3* and *4*), whereas constructs that lack the NRM no longer bound to the Nup82p-Nsp1p-Nup159p complex (Fig. 2*B*, *lanes 1* and *2*). Thus, a relatively short sequence within the Nup116p C-terminal domain, which includes the NRM, is sufficient for interaction with the Nup82p complex.

Human NUP98 Interacts with the Yeast Nup82p Complex—Human NUP98 is the putative higher eucaryotic homologue of Nup116p and contains a GLEBS in its N-terminal domain that mediates binding to GLE2/RAE1 and an NRM in its C-terminal part. To find out whether human NUP98 can interact with the Nup82p complex, we expressed ProtA-NUP98-C in yeast and affinity-purified it by IgG-Sepharose chromatography (Fig. 2*C*). Clearly, the three members of the Nup82p complex could be detected in the ProtA-NUP98-C eluate by Western analysis, whereas other nucleoporins such as Nic96p (Fig. 2*C*, *lane 2*) and Nup157p (data not shown) were absent. Thus, the interaction of Nup116p/NUP98 with the Nup82p complex appears to be conserved during evolution.

Nup116p Localizes to the Cytoplasmic Side of the Nuclear Pore Complex—To study the localization of Nup116p within the structural framework of the NPC, ProtA-Nup116p and ProtA-Nup116p-C were analyzed by pre-embedding immunogold labeling (13). This revealed that both full-length Nup116p and Nup116p-C were predominantly located on the cytoplasmic side of the NPC at average distances of 39 and 33 nm, respectively, from the central plane (Fig. 3). Quantitative analysis showed that 91.4 and 96.4% of gold, indicating ProtA-Nup116p and ProtA-Nup116p-C, respectively, were found on the cyto-

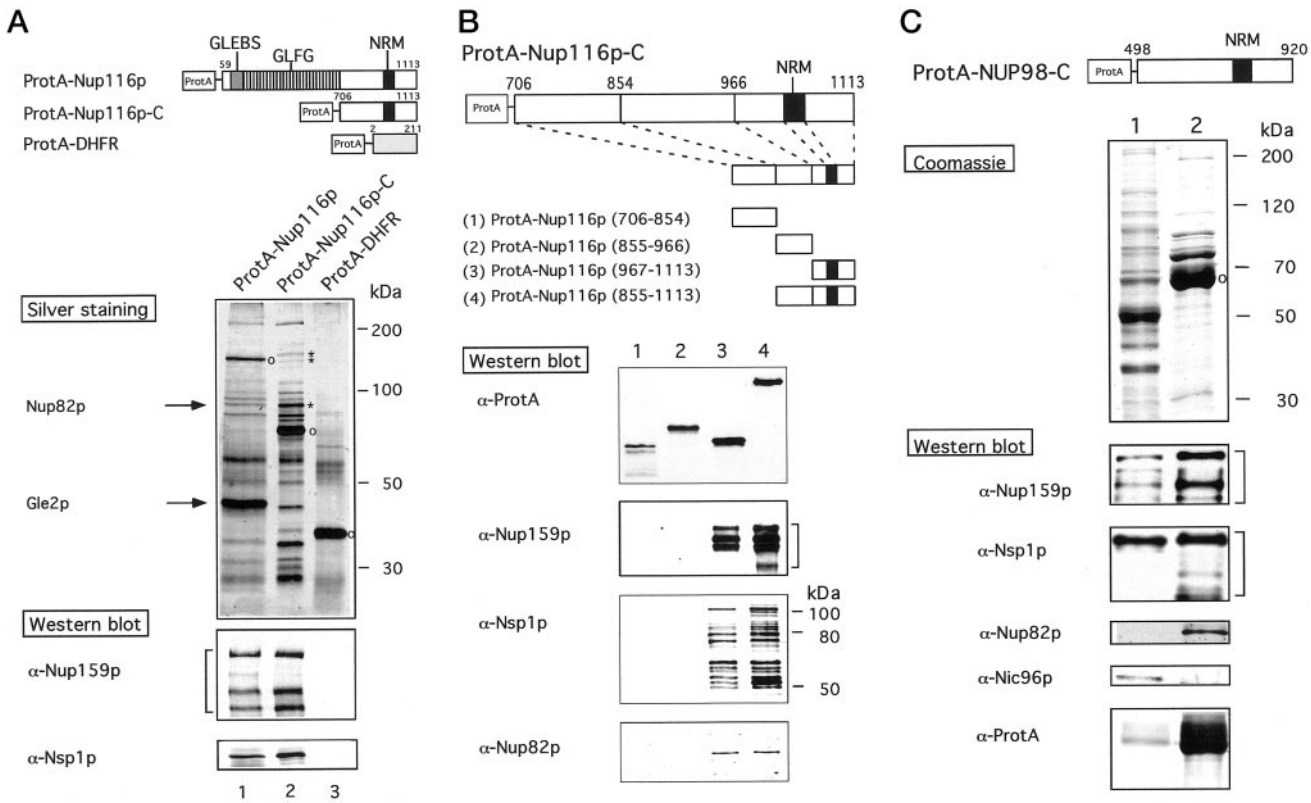

FIG. 2. **Yeast Nup116p and human NUP98 interact with Nup82p via the NRM domain.** *A*, affinity purification of ProtA-Nup116p, ProtA-Nup116p-C, and ProtA-tagged dihydrofolate reductase (*DHFR*). The eluted ProtA fusion proteins were analyzed by SDS-PAGE and silver staining or by Western blotting using anti-Nup159p or anti-Nsp1p antibodies. The positions of the ProtA fusion proteins are indicated by *circles*. Both Nup159p and Nsp1p are highly sensitive to proteolysis, leading to many breakdown products detected on the Western blot. *B*, the sequence around the NRM of Nup116p is sufficient for association with the Nup82p complex. *Upper panel*, *schematic* of Nup116p-C and its various truncation constructs (*1–4*); *lower panel*, affinity purification of the Nup116p-C deletion constructs from the *nup116*Δ strain. The eluates were analyzed by SDS-PAGE and Western blotting using the indicated antibodies. *C*, human NUP98 associates with the Nup82p complex. ProtA-NUP98-C including the NRM was expressed in the BJ2168 protease-deficient strain and affinity-purified by IgG-Sepharose chromatography. A whole cell lysate (*lane 1*) and the eluate from the IgG column (*lane 2*) were analyzed by SDS-PAGE and Coomassie staining or by Western blotting using the indicated antibodies. ProtA-NUP98-C is indicated by a *circle*; the prominent bands above most likely represent heat shock proteins.

plasmic fibrils, and only 8.3 and 3.6%, respectively, at the nucleoplasmic face of the NPC (data not shown). By immunogold labeling, Nup82p and Nup159p were recently found on the cytoplasmic side of the nuclear pore complex at an average of 30 nm from its central plane (13, 20, 23).

Physical Interaction of Nup116p-C with the Nup82p Complex Is Impaired in the nup82-27 Mutant—To find out whether mutant alleles of *NUP82* affect the physical interaction with the Nup116p C-terminal domain, we tagged the *nup82-27* allele with GFP or ProtA to facilitate subcellular location studies or biochemical purification (Fig. 4). *nup82-27* is a novel thermosensitive allele that was isolated by random PCR mutagenesis (see "Materials and Methods"). GFP-tagged *nup82-27* was able to complement the *nup82* null mutant at 30 °C, but not at 37 °C (Fig. 4*A*). Like other *nup82* mutants, *nup82-27* showed nuclear accumulation of poly(A)$^+$ RNA when shifted to 37 °C for 1–2 h (Fig. 4*B*). To monitor the interaction of GFP-tagged *nup82-27* with the NPC, *nup82*Δ cells expressing GFP-*nup82-27* were analyzed by fluorescence microscopy at 23 °C or after a 2-h shift to 37 °C (Fig. 4*C*). When grown on plates at the permissive temperature, GFP-*nup82-27* cells showed nuclear envelope staining, but not as distinct as that shown by GFP-Nup82p cells (data not shown). In contrast, exponentially growing GFP-*nup82-27* cells had largely lost the ring-like staining both at 23 and 37 °C (Fig. 4*C*). This suggests that the *nup82-27* mutation affects the steady-state nuclear envelope location of Nup82p.

When GFP-tagged Nup116p or Nup159p was analyzed in *nup82-27* cells, they still exhibited nuclear envelope staining when the cells were grown at 23 °C (data not shown), but after shifting to 37 °C for 2 h, GFP-Nup159p was no longer detected at the nuclear envelope, whereas GFP-Nup116p remained associated with the NPCs (Fig. 4*D*). As a control, *NUP82* and *nup82-27* cells were transformed with GFP-Nic96p, which exhibited a normal NPC distribution at both temperatures. Thus, association of Nup159p and Nup82p with the nuclear pores is impaired in the *nup82-27* mutant, whereas Nup116p still associates with the nuclear envelope.

We next wanted to find out whether ProtA-Nup82p is able to co-isolate Nup116p and whether the physical interaction between Nup116p and Nup82p is altered in a *nup82* mutant. Therefore, ProtA-tagged *nup82-27* was affinity-purified from a *nup82* disruption strain also expressing Myc-tagged Nup116p-C. When affinity-purified from cells grown at 23 °C, ProtA-*nup82-27* co-isolated a fraction of Myc-tagged Nup116p-C together with Nsp1p and Nup159p (Fig. 4*E*, *lane 1*). Following a temperature shift to 37 °C, association of Myc-Nup116p-C with ProtA-*nup82-27* was lost (Fig. 4*E*, *lane 2*), and only small amounts of Nup159p and Nsp1p copurified. This indicates that the Nup82p complex derived from the *nup82-27* strain is biochemically unstable. Taken together, at the restrictive temperature, Nup116p remains associated with the NPCs in the *nup82-27* mutant, but its interaction with the mutant Nup82p-Nsp1p-Nup159p complex is largely lost (see "Discussion").

Nup116p Functionally Interacts with All Members of the Nup82p Complex—Our data revealed a so far not recognized interaction between Nup116p and the Nup82p complex. This could be of func-

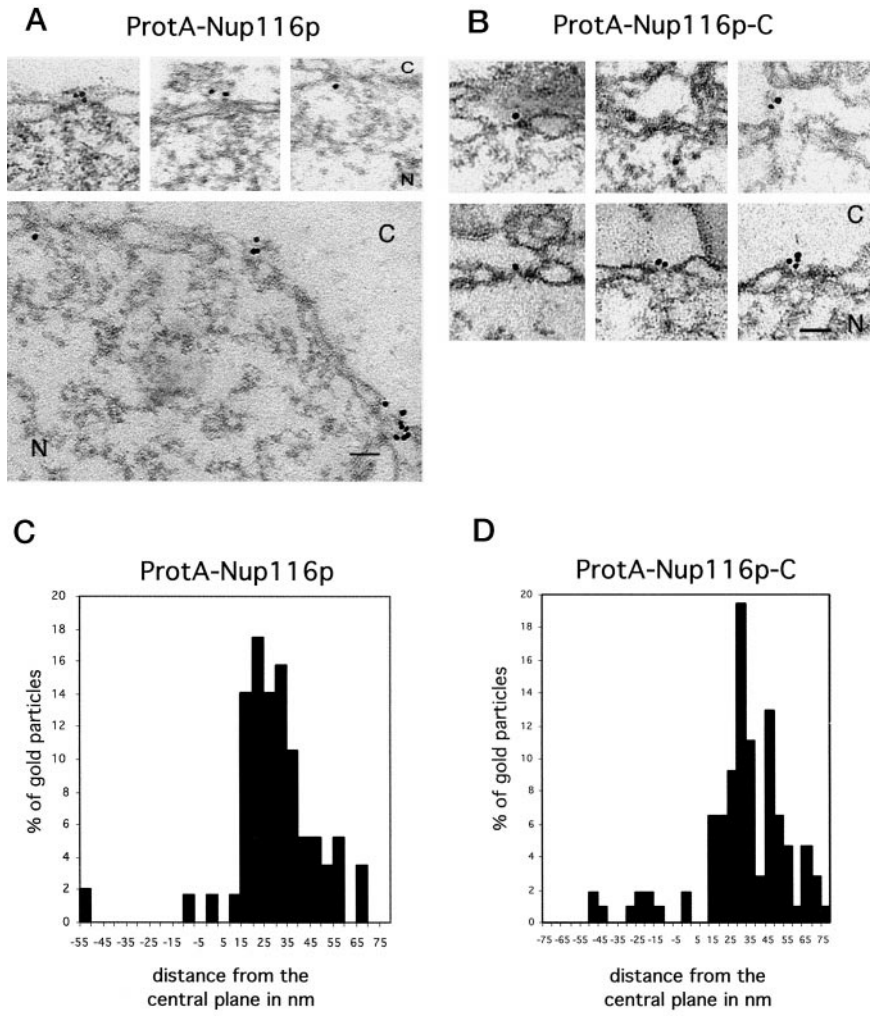

FIG. 3. **Immunoelectron microscopy of yeast strains expressing ProtA-Nup116p and ProtA-Nup116p-C.** Shown are nuclear envelope cross-sections with adjacent nucleoplasm (*N*) and cytoplasm (*C*) from Triton X-100-extracted *nup116Δ(URA3)* cells expressing ProtA-Nup116p (*A*) or ProtA-Nup116p-C (*B*). Cells were labeled with gold-conjugated anti-ProtA antibodies using a preembedding method. A gallery of representative photographs is shown. The results from the quantitative analysis of the distance of ProtA-Nup116p (*C*) and ProtA-Nup116p-C (*D*) from the central plane are also shown. *Scale bars* = 100 nm.

tional relevance for nucleocytoplasmic transport since both subcomplexes, the Nup116p-Gle2p and Nup82p-Nsp1p-Nup159p complex, are involved in nuclear mRNA export. To test for a functional overlap, genetic interactions were tested between members of these two subcomplexes. Since a *nup116*Δ strain is viable at 30 °C (but is temperature-sensitive at 37 °C), haploid strains *nsp1*Δ/*nup116*Δ, *nup82*Δ/*nup116*Δ, and *nup159*Δ/*nup116*Δ expressing different alleles of *NSP1*, *NUP82*, and *NUP159* were constructed. They were then tested for synergistic growth defects at 23 °C by plating cells on 5-fluoroorotic acid-containing plates (Fig. 5, *schematic*). In the past, our laboratory has identified *NUP116* based on its synthetically lethal interaction with the *nsp1-L640S* allele, which maps to the C-terminal domain of Nsp1p (34). We now show in a distinct way that the *nsp1-L640S* allele is synthetically lethal with the *nup116*Δ allele (Fig. 5*A*). The same was found for the *nsp1-ala6* allele, which encodes another mutation within the Nsp1p C-terminal domain that affects both Nsp1p subcomplexes (Ref. 19 and data not shown). To find out which of the Nup116p domains contributes to the observed synthetic lethality with *NSP1*, the *nup116-C*, *nup116ΔC*, *nup116ΔGLEBS*, and *nup116ΔNRM* constructs were expressed in the nonviable *nup116*Δ/*nsp1-L640S* strain (Fig. 5*A*; for definition of these constructs, see the figure legend). Unexpectedly, the lack of the C-terminal domain of Nup116p was not the cause for synthetic lethality with *nsp1-L640S*. In fact, it was the GLEBS that genetically interacted with *NSP1* since its deletion created synthetic lethality with *nsp1-L640S* (Fig. 5*A*, *nup116ΔGLEBS*). This points to a functional overlap between Nsp1p and Gle2p.

Since Nsp1p is part of two subcomplexes (see above), results derived from the synthetic lethal interactions between *nup116* and *nsp1* mutant alleles may be difficult to interpret. We therefore analyzed synthetic lethal relationships between *nup116* mutant alleles and either *nup82* or *nup159* alleles. As anticipated, combining the *nup116*Δ and *nup82-27* alleles caused synthetic lethality, which could be fully complemented by the expression of the Nup116p C-terminal domain (Fig. 5*B*). Accordingly, deletion of the entire Nup116p C terminus or a shorter fragment containing the NRM resulted in synthetic lethality (Fig. 5*B*). These findings are consistent with the biochemical data that showed that (i) *nup82-27* is impaired in its physical interaction with Nup116p-C (see also Fig. 4*E*) and (ii) a C-terminal sequence of Nup116p containing the NRM is sufficient for interaction with the Nup82p complex (see also Fig. 3*C*). Notably, a *nup82*Δ/*nup100*Δ strain expressing Myc-*nup82-27* was viable, although it grew slower than a *nup82-27* strain (Fig. 5*D*). Thus, biochemical data and genetic data complement each other in the sense that predominantly, ProtA-Nup116p-C, but not ProtA-Nup100p-C, stably interacts with the Nup82p complex.

Finally, we tested for genetic interactions between different *nup159* and *nup116* mutant alleles. As shown previously, deletion of the N-terminal part of Nup159p (*nup159ΔN*), both the N-terminal and FG repeat domains (*nup159-C*), or part of the coiled-coil C-terminal domain (*nup159-1*/*rat7-1*) causes temperature-sensitive growth concomitant with defects in nuclear poly(A)$^+$ RNA export (Refs. 22 and 55; see also Fig. 5*C*, +*NUP116*). Furthermore, mutations in the C-terminal coiled-coil region of Nup159p affect the integrity of the Nup82p com-

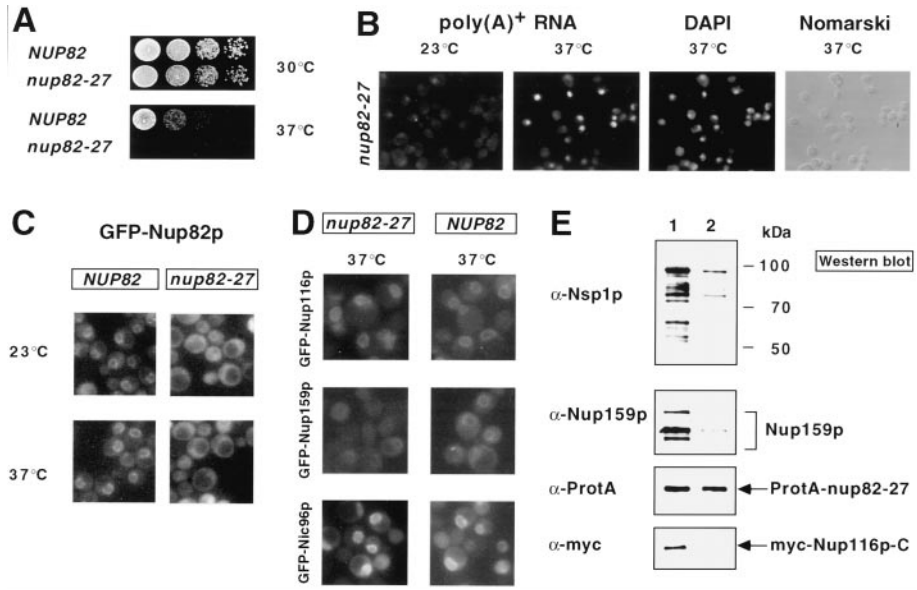

FIG. 4. **Characterization of the *nup82-27* temperature-sensitive allele.** *A*, the *nup82-27* mutant allele was generated by PCR mutagenesis. The growth properties of *nup82*Δ cells complemented by GFP-Nup82p or GFP-*nup82-27* were compared on YPD plates at 30 and 37 °C. *B*, shown is the poly(A)$^+$ RNA localization in *nup82-27* cells. To detect mRNA export defects, *nup82*Δ cells expressing ProtA-*nup82-27* were grown at 23 °C before shifting them to 37 °C for 3 h. The localization of poly(A)$^+$ RNA was analyzed by *in situ* hybridization with a Cy3-labeled oligo(dT) probe. DNA was visualized by 4,6-diamidino-2-phenylindole (*DAPI*) staining; a Nomarski picture of cells grown at 37 °C is shown. *C*, shown is the nuclear envelope location of GFP-Nup82p or GFP-*nup82-27* in *nup82*Δ cells as revealed by fluorescence microscopy. Cells were grown in selective SD medium at 23 °C or shifted to 37 °C for 3 h. *D*, shown is the localization of GFP-Nup116p, GFP-Nup159p, and GFP-Nic96p in *NUP82* and *nup82-27* cells. Cells were grown in liquid medium at 23 °C or shifted to 37 °C for 2 h. *E*, shown is the physical interaction of Nup116p-C with the Nup82p complex in the *nup82-27* mutant. The *nup82*Δ strain complemented by ProtA-*nup82-27* expressed a Myc-tagged version of Nup116p-C. The cells were grown at 23 °C before being shifted to 37 °C for 3 h. After affinity purification, eluates were analyzed by SDS-PAGE and Western blotting. Proteins were identified by the antibodies indicated. Eluates were derived from cells grown at 23 °C (*lane 1*) and 37 °C (*lane 2*).

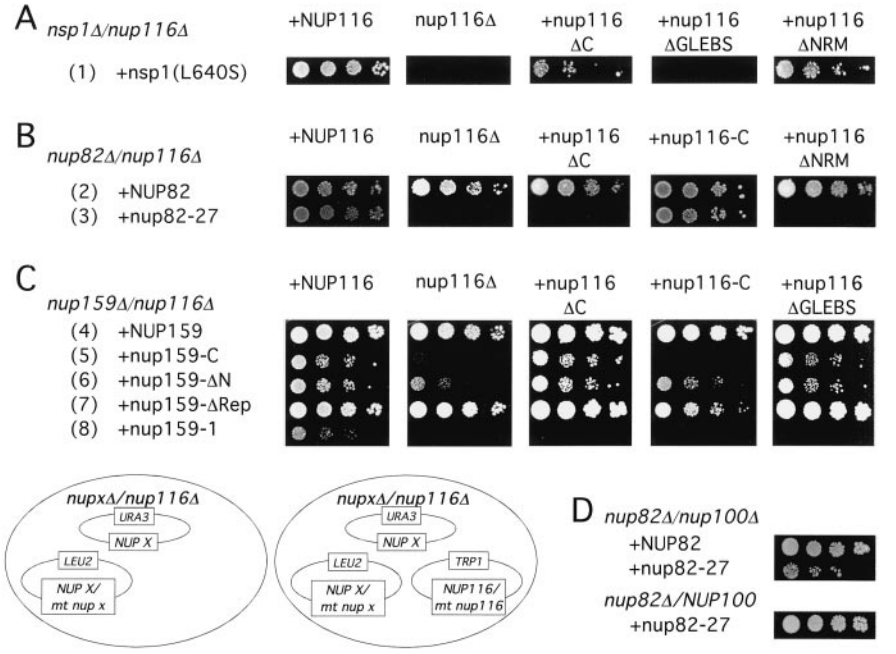

FIG. 5. ***NUP116* interacts genetically with all members of the Nup82p-Nsp1p-Nup159p complex.** The double disruption strains *nsp1*Δ/*nup116*Δ (*A*), *nup82*Δ/*nup116*Δ (*B*), *nup159*Δ/*nup116*Δ (*C*), and *nup82*Δ/*nup100*Δ (*D*) were transformed with plasmids encoding the indicated wild-type or mutant proteins. Precultures were diluted in 10^{-1} steps, and equivalent amounts of cells were dropped on 5-fluoroorotic acid plates and grown at 23 °C for 8 days. The plasmids (*ARS*/*CEN*) *NUP116*, *nup116-C*, *nup116*Δ*C*, *nup116*Δ*GLEBS*, and *nup116*Δ*NRM* contained the *TRP1* gene. The plasmids *nsp1-L640S*, *NUP82*, *nup82-27*, *NUP159*, *nup159-C*, *nup159*Δ*N*, *nup159*Δ*Rep*, and *nup159-1* in *A–C* carried the *LEU2* gene. The plasmids *NUP82* and *nup82-27* shown in *D* carried the *TRP1* gene. All plasmids are described under "Materials and Methods."

plex (19). When we tested for synthetic lethality, a complex relationship was found between the various Nup159p and Nup116p domains (Fig. 5*C*), *e.g.* both the Nup159p C- and N-terminal domains genetically overlapped with Nup116p (Fig. 5*C*, *nup116*Δ). In contrast, deletion of the FG repeat domain of Nup159p (*nup159*Δ*Rep*) did not cause synthetic lethality with *nup116*Δ. Interestingly, the *nup116-C* allele (lacking the GLFG and GLEBS domains) did not complement synthetic lethality when either the Nup159p C-terminal domain (*nup159-C*) or the Nup159p N-terminal and FG (*rat7-1*) domains were present (Fig. 5*C*). We conclude that Nup116p is composed of at least three functionally different regions, the

GLEBS, GLFG, and NRM domains, all of which overlap genetically in a complex way with all members of the Nup82p-Nsp1p-Nup159p complex.

DISCUSSION

When we started our genetic analysis of the yeast nuclear pore complex several years ago using *NSP1* as the first bait in synthetic lethal screens, we frequently found *nup116* mutants to be synthetically lethal with the *nsp1-L640S* temperature-sensitive allele; yet we were not able to show that Nup116p physically interacts with Nsp1p (34). This contrasted with the finding that Nup49p, Nup57p, and Nic96p, which were also found in genetic screens with the same *nsp1-L640S* allele (yet with lower frequency), form a biochemically stable complex with Nsp1p (the Nsp1p-Nup49p-Nup57p-Nic96p complex). Nevertheless, the possibility remained that Nsp1p and Nup116p only functionally overlap (*i.e.* are involved in the same or overlapping pathways) without coming into physical contact. Our data presented here now show for the first time that the Nup116p-Gle2p complex gains physical contact with Nsp1p in the form of the Nup82p-Nsp1p-Nup159p complex and thus explain our former genetic data.

The first indication that Nup116p physically associates with the Nup82p complex was obtained from mass spectrometry; a distinct silver-stainable band found in the affinity-purified ProtA-Nup116p-C eluate was thereby identified to be Nup82p, whereas several weaker bands were breakdown products of Nup159p. Since Nup82p, Nup159p, and Nsp1p form a distinct NPC subcomplex (18–20), we performed Western blot analysis to show that Nsp1p is also associated with Nup116p-C. The co-isolation of Nup116p and a pool of Nsp1p was best seen when the C-terminal domain of Nup116p was used as affinity ligand, but also when full-length Nup116p together with Gle2p bound to the Nup82p-Nsp1p-Nup159p complex. Interestingly, an even shorter part within the Nup116p carboxyl-terminal domain that includes the NRM (a conserved sequence that can bind to homopolymeric RNA *in vitro*; see Ref. 38) was sufficient for stable complex formation. The absence of other known nucleoporins like Nic96p in the affinity-purified ProtA-Nup116p-C-Nup82p complex indicates that the interaction between Nup116p and the Nup82p complex is specific. However, so far, we have been unable to show a direct interaction between Nup116p-C and any protein of the Nup82p complex. Thus, we cannot rule out that RNA or other proteins yet to be identified are involved in this interaction. In agreement with our biochemical data, we have localized ProtA-Nup116p and ProtA-Nup116p-C predominantly to the cytoplasmic side of the NPC in close proximity to the sites where Nup159p and Nup82p were found before (13, 20, 23).

Previous studies point to a role of Nup116p and its associated Gle2p in nuclear mRNA transport (36, 43). Several other proteins involved in RNA transport and metabolism were also found in physical and/or functional interaction with the Nup82p complex or its putative higher eucaryotic counterpart, CAN/NUP214-NUP88-p66 (25), among them the yeast mRNA export factors Mex67p (28) and Gle1p (20, 32), the export factor CRM1 (25), and the RNA helicase Dbp5p (29, 30). Interestingly, *gle1* mutants are synthetically lethal with a *nup116* and a *nup100* null mutation, pointing to a functional network between Gle1p, the Nup82p complex, and the Nup116p complex. Here we show that a *nup116* null disruption is synthetically lethal with C-terminal mutations of *NUP159*, *NUP82*, or *NSP1*, which all affect the integrity of the Nup82p-Nsp1p-Nup159p subcomplex. Nup116p-C complements only the *nup82* mutant, but not the *nup159* and *nsp1* mutants, which could indicate a specific function shared by Nup82p and Nup116p-C. Another genetic overlap exists between the GLFG region of Nup116p and the N-terminal and FG repeat domains of Nup159p. Whether these domains perform a redundant function with any of the above-mentioned proteins (*e.g.* providing docking sites for shuttling transport receptors) and thereby cooperate during nuclear mRNA and protein export remains to be shown. Our recent finding shows a strong genetic and physical interaction between the Mex67p-Mtr2p complex and Nup116p GLFG repeat sequences, suggesting that Nup116p is one of the targets within the structural framework of the NPC with which this essential mRNA export complex interacts.[3]

Nup116p, Nup100p, and Nup145p-N are three GLFG nucleoporins that show a high degree of similarity and redundancy, particularly within their NRM regions (35–38). It is therefore surprising that only Nup116p-C, but not the C-terminal parts of Nup100p and Nup145p-N, interacts with the Nup82p complex. As a possible explanation, Nup100p-C and Nup145p-NΔGLFG may be more loosely attached to the Nup82p complex and therefore are lost during purification. Alternatively, Nup116p could predominantly interact with the Nup82p complex compared with Nup100p-C and Nup145p-NΔGLFG. Finally, other functional domains within Nup100p and Nup145p-N may target these proteins (also) to different sites within the NPC, thus preventing a stable physical contact with the Nup82p complex. In this context, it is worth mentioning that affinity-purified Nup145p-NΔGLFG contained significant amounts of Nup157p (as measured by mass spectrometry), a member of the Nup170p-Nup157p-Nup188p complex (8–10). Thus, Nup145p-N could participate preferentially in a pathway in which the Nup170p-Nup157p-Nup188p complex also operates. We also observed that a *gle2*Δ/*nup100*Δ strain is complemented by *NUP100-C* or *NUP116-C*, but not by *NUP145-NΔGLFG*.[4] This also points to a functional difference between Nup116p-C, Nup100p-C, and Nup145p-NΔGLFG.

Expression of ProtA-tagged human NUP98-C in yeast revealed that NUP98 associates with the Nup82p complex. Thus, the assumed evolutionary conservation between Nup116p and NUP98 is also seen at the level of physical interaction with the nearest neighbors. Based on these results, one may find a physical association of the NUP98-RAE1 complex with the CAN/NUP214-NUP88-p66 complex in higher eucaryotes (24, 25, 50). In contrast to Nup116p, which is found on the cytoplasmic fibrils, NUP98 was previously located on the nucleoplasmic side of the NPC (48). This may indicate that NUP98 is not confined to a certain area within the NPC. In fact, it was shown that NUP98 and its interacting RAE1 shuttle between the nucleus and cytoplasm (50, 51, 52). In analogy to NUP98, it is thus conceivable that Nup116p is able to move between nuclear and cytoplasmic compartments or between the cytoplasmic and nuclear phases of the NPC. Our observation that Nup116p is located at the nuclear periphery independently of the Nup82p complex could thus indicate that only a certain pool of Nup116p forms a complex with the Nup82p-Nsp1p-Nup159p complex, whereas at the same time, it could perform a role in the association with other nucleoporins, *e.g.* on the nucleoplasmic side of the NPC.

In summary, we have shown for the first time a higher order assembly between the Nup116p-Gle2p and Nup82p-Nsp1p-Nup159p complexes. Both subcomplexes seem to perform important functions in nuclear mRNA export. That both complexes are now found to come into physical contact suggests an mRNA export route in which these complexes, either in concert or serially, hand over shuttling mRNA export factors such as the Mex67p-Mtr2p complex.

[3] Sträßer, K., Baßler, J., and Hurt, E. (2000) *J. Cell Biol.*, in press.
[4] S. M. Bailer, unpublished data.

Acknowledgments—We thank C. Cole for kindly providing polyclonal antibodies against Nup159p, the *NUP159* shuffle strain, and plasmids encoding wild-type Nup159p and Nup159p mutants. The cDNA encoding human NUP98 was kindly provided by Jan van Deursen (Mayo Clinic, Rochester, MN). J. Aris provided antibodies against Nsp1p. We are also grateful to members of our laboratory, especially Drs. George Simos and Buket Kosova, for critically reading the manuscript.

REFERENCES

1. Stoffler, D., Fahrenkrog, B., and Aebi, U. (1999) *Curr. Opin. Cell Biol.* **11,** 391–401
2. Doye, V., and Hurt, E. (1997) *Curr. Opin. Cell Biol.* **9,** 401–411
3. Gorlich, D., and Kutay, U. (1999) *Annu. Rev. Cell Dev. Biol.* **15,** 607–660
4. Aitchison, J. D., Blobel, G., and Rout, M. P. (1995) *J. Cell Biol.* **131,** 1659–1675
5. Goldstein, A. L., Snay, C. A., Heath, C. V., and Cole, C. N. (1996) *Mol. Biol. Cell* **7,** 917–934
6. Siniossoglou, S., Wimmer, C., Rieger, M., Doye, V., Tekotte, H., Weise, C., Emig, S., Segref, A., and Hurt, E. C. (1996) *Cell* **84,** 265–275
7. Teixeira, M. T., Siniossoglou, S., Podtelejnikov, S., Benichou, J. C., Mann, M., Dujon, B., Hurt, E., and Fabre, E. (1997) *EMBO J.* **16,** 5086–5097
8. Nehrbass, U., Rout, M. P., Maguire, S., Blobel, G., and Wozniak, R. W. (1996) *J. Cell Biol.* **133,** 1153–1162
9. Zabel, U., Doye, V., Tekotte, H., Wepf, R., Grandi, P., and Hurt, E. C. (1996) *J. Cell Biol.* **133,** 1141–1152
10. Marelli, M., Aitchison, J. D., and Wozniak, R. W. (1998) *J. Cell Biol.* **143,** 1813–1830
11. Grandi, P., Schlaich, N., Tekotte, H., and Hurt, E. C. (1995) *EMBO J.* **14,** 76–87
12. Bucci, M., and Wente, S. R. (1997) *J. Cell Biol.* **136,** 1185–1199
13. Fahrenkrog, B., Hurt, E. C., Aebi, U., and Pante, N. (1998) *J. Cell Biol.* **143,** 577–488
14. Dabauvalle, M. C., Loos, K., and Scheer, U. (1990) *Chromosoma* (*Berl.*) **100,** 56–66
15. Finlay, D. R., Meier, E., Bradley, P., Horecka, J., and Forbes, D. J. (1991) *J. Cell Biol.* **114,** 169–183
16. Hu, T., Guan, T., and Gerace, L. (1996) *J. Cell Biol.* **134,** 589–601
17. Grandi, P., Dang, T., Pante, N., Shevchenko, A., Mann, M., Forbes, D., and Hurt, E. (1997) *Mol. Biol. Cell* **8,** 2017–2038
18. Grandi, P., Emig, S., Weise, C., Hucho, F., Pohl, T., and Hurt, E. C. (1995) *J. Cell Biol.* **130,** 1263–1273
19. Belgareh, N., Snay-Hodge, C., Pasteau, F., Dagher, S., Cole, C. N., and Doye, V. (1998) *Mol. Biol. Cell* **9,** 3475–3492
20. Hurwitz, M. E., Strambio-de-Castillia, C., and Blobel, G. (1998) *Proc. Natl. Acad. Sci. U. S. A.* **95,** 11241–11245
21. Hurwitz, M. E., and Blobel, G. (1995) *J. Cell Biol.* **130,** 1275–1281
22. Del Priore, V., Heath, C., Snay, C., MacMillan, A., Gorsch, L., Dagher, S., and Cole, C. (1997) *J. Cell Sci.* **110,** 2987–2999
23. Kraemer, D. M., Strambio-de-Castillia, C., Blobel, G., and Rout, M. P. (1995) *J. Biol. Chem.* **270,** 19017–19021
24. Bastos, R., Ribas de Pouplana, L., Enarson, M., Bodoor, K., and Burke, B. (1997) *J. Cell Biol.* **137,** 989–1000
25. Fornerod, M., van Deursen, J., van Baal, S., Reynolds, A., Davis, D., Murti, K. G., Fransen, J., and Grosveld, G. (1997) *EMBO J.* **16,** 807–816
26. Segref, A., Sharma, K., Doye, V., Hellwig, A., Huber, J., Luhrmann, R., and Hurt, E. (1997) *EMBO J.* **16,** 3256–3271
27. Santos-Rosa, H., Moreno, H., Simos, G., Segref, A., Fahrenkrog, B., Pante, N., and Hurt, E. (1998) *Mol. Cell. Biol.* **18,** 6826–6838
28. Katahira, J., Sträßer, K., Podtelejnikov, A., Mann, M., Jung, J. U., and Hurt, E. (1999) *EMBO J.* **18,** 2593–2609
29. Hodge, C. A., Colot, H. V., Stafford, P., and Cole, C. N. (1999) *EMBO J.* **18,** 5778–5788
30. Schmitt, C., von Kobbe, C., Bachi, A., Pante, N., Rodrigues, J. P., Boscheron, C., Rigaut, G., Wilm, M., Seraphin, B., Carmo-Fonseca, M., and Izaurralde, E. (1999) *EMBO J.* **18,** 4332–4347
31. Murphy, R., and Wente, S. R. (1996) *Nature* **383,** 357–360
32. Del Priore, V., Snay, C. A., Bahr, A., and Cole, C. N. (1996) *Mol. Biol. Cell* **7,** 1601–1621
33. Strahm, Y., Fahrenkrog, B., Zenklusen, D., Rychner, E., Kantor, J., Rosbach, M., and Stutz, F. (1999) *EMBO J.* **18,** 5761–5777
34. Wimmer, C., Doye, V., Grandi, P., Nehrbass, U., and Hurt, E. C. (1992) *EMBO J.* **11,** 5051–5061
35. Wente, S. R., Rout, M. P., and Blobel, G. (1992) *J. Cell Biol.* **119,** 705–723
36. Wente, S. R., and Blobel, G. (1993) *J. Cell Biol.* **123,** 275–284
37. Wente, S. R., and Blobel, G. (1994) *J. Cell Biol.* **125,** 955–969
38. Fabre, E., Boelens, W. C., Wimmer, C., Mattaj, I. W., and Hurt, E. C. (1994) *Cell* **78,** 275–289
39. Iovine, M. K., Watkins, J. L., and Wente, S. R. (1995) *J. Cell Biol.* **131,** 1699–1713
40. Iovine, M. K., and Wente, S. R. (1997) *J. Cell Biol.* **137,** 797–811
41. Bailer, S. M., Siniossoglou, S., Podtelejnikov, A., Hellwig, A., Mann, M., and Hurt, E. (1998) *EMBO J.* **17,** 1107–1119
42. Ho, A. K., Raczniak, G. A., Ives, E. B., and Wente, S. R. (1998) *Mol. Biol. Cell* **9,** 355–373
43. Murphy, R., Watkins, J. L., and Wente, S. R. (1996) *Mol. Biol. Cell* **7,** 1921–1937
44. Sarkar, S., and Hopper, A. K. (1998) *Mol. Biol. Cell* **9,** 3041–3055
45. Brown, J. A., Bharathi, A., Ghosh, A., Whalen, W., Fitzgerald, E., and Dhar, R. (1995) *J. Biol. Chem.* **270,** 7411–7419
46. Whalen, W. A., Bharathi, A., Danielewicz, D., and Dhar, R. (1997) *Yeast* **13,** 1167–1179
47. Powers, M. A., Macaulay, C., Masiarz, F. R., and Forbes, D. J. (1995) *J. Cell Biol.* **128,** 721–736
48. Radu, A., Moore, M. S., and Blobel, G. (1995) *Cell* **81,** 215–222
49. Powers, M. A., Forbes, D. J., Dahlberg, J. E., and Lund, E. (1997) *J. Cell Biol.* **136,** 241–250
50. Pritchard, C. E., Fornerod, M., Kasper, L. H., and van Deursen, J. M. (1999) *J. Cell Biol.* **145,** 237–254
51. Zolotukhin, A. S., and Felber, B. K. (1999) *J. Virol.* **73,** 120–127
52. Kraemer, D., and Blobel, G. (1997) *Proc. Natl. Acad. Sci. U. S. A.* **94,** 9119–9124
53. Emtage, J. L., Bucci, M., Watkins, J. L., and Wente, S. R. (1997) *J. Cell Sci.* **110,** 911–925
54. Hurt, E. C. (1988) *EMBO J.* **7,** 4323–4334
55. Gorsch, L. C., Dockendorff, T. C., and Cole, C. N. (1995) *J. Cell Biol.* **129,** 939–955
56. Muhlrad, D., Hunter, R., and Parker, R. (1992) *Yeast* **8,** 79–82
57. Vartanian, J. P., Henry, M., and Wain-Hobson, S. (1996) *Nucleic Acids Res.* **24,** 2627–2631
58. Maniatis, T., Fritsch, E. F., and Sambrook, J. (1982) *Molecular Cloning: A Laboratory Manual*, Cold Spring Harbor Laboratory, Cold Spring Harbor, NY
59. Aris, J. P., and Blobel, G. (1988) *J. Cell Biol.* **107,** 17–31
60. Nehrbass, U., Fabre, E., Dihlmann, S., Herth, W., and Hurt, E. C. (1993) *Eur. J. Cell Biol.* **62,** 1–12